haematologica
Journal of the Ferrata Storti Foundation

Depletion of the RNA binding protein QKI and circular RNA dysregulation in T-cell acute lymphoblastic leukemia

by Alessia Buratin, Bruno Palhais, Enrico Gaffo, Juliette Roels, Julie Morscio, Jolien Van Laere, Silvia Orsi, Geertruij te Kronnie, Pieter Van Vlierberghe, Panagiotis Ntziachristos, and Stefania Bortoluzzi

Received: May 30, 2024.
Accepted: November 25, 2024.

Citation: Alessia Buratin, Bruno Palhais, Enrico Gaffo, Juliette Roels, Julie Morscio, Jolien Van Laere, Silvia Orsi, Geertruij te Kronnie, Pieter Van Vlierberghe, Panagiotis Ntziachristos, and Stefania Bortoluzzi. Depletion of the RNA binding protein QKI and circular RNA dysregulation in T-cell acute lymphoblastic leukemia.
Haematologica. 2024 Dec 5. doi: 10.3324/haematol.2024.285971 [Epub ahead of print]

Depletion of the RNA binding protein QKI and circular RNA dysregulation in T-cell acute lymphoblastic leukemia

Alessia Buratin[1], Bruno Palhais[2,3,4], Enrico Gaffo[1], Juliette Roels[4], Julie Morscio[4], Jolien Van Laere[4], Silvia Orsi[1,5], Geertruij te Kronnie[1], Pieter Van Vlierberghe[4], Panagiotis Ntziachristos[2,3,4] and Stefania Bortoluzzi[1*]

[1] Department of Molecular Medicine, University of Padova, Padova, Italy

[2] Leukemia Therapy Resistance Unit, Department of Biomolecular Medicine, Ghent University, Ghent, Belgium.

[3] Center for Medical Genetics, Ghent University and University Hospital, Ghent, Belgium.

[4] Cancer Research Institute Ghent (CRIG), Ghent, Belgium

[5] Department of Biology, University of Padova, Padova, Italy

***Correspondence:** Prof. Stefania Bortoluzzi, Department of Molecular Medicine, University of Padova, via G. Colombo 3, 35131- Padova, Italy. Email: stefania.bortoluzzi@unipd.it

Short Title

QKI Expression and circRNA Dysregulation in T-ALL

Acknowledgements

SB is supported by Fondazione AIRC per la Ricerca sul Cancro (IG 2017 #20052 and IG#2023 #28966) to SB, EU funding within the MUR PNRR “National Center for Gene Therapy and Drugs based on RNA Technology” (Project no. CN00000041 CN3 Spoke #6 "RNA chemistry") and “National Center for HPC, Big Data and Quantum Computing” (Project no. CN00000013 CN1 Spoke #8 "In Silico Medicine & Omics Data"), PRIN MIUR 2017 #2017PPS2X4_003 and PRIN MIUR 2022 #20222EC7LA. PN is supported by the Research Foundation Flanders (FWO,

G0F4721N and G0A8B24N), start-up funds from the Department of Biomolecular Medicine, Ghent University, a Flanders interuniversity consortium grant (BOF.IBO.2023.0006.02) and a Cancer Research Institute Ghent (CRIG) partnership grant.

Author Contributions

AB, GTK, PVV and SB conceived the study. AB and SB were responsible for data selection, bioinformatic analysis and results interpretation. EG provided software. BP, EG, JR and SO collaborated on bioinformatic analyses. BP, JM, and JVL performed experiments. PN And SB supervised the project. AB, BP and SB wrote the manuscript. EG, GTK and PN revised the manuscript and all authors approved it.

Competing Interests

None to disclose.

Data Availability Statement

RNA-seq data (GSE110636 and GSE142179) are freely available at Gene Expression Omnibus (https://www.ncbi.nlm.nih.gov/geo/).

This study investigates the impact of abnormally low QKI expression on T-ALL circRNAome.

Circular RNAs (circRNAs) drive oncogenic processes, acting as both oncogenic and tumor suppressor molecules[1]. Recent data on aberrant circRNA expression and functional impact in T-cell Acute Lymphoblastic Leukemia (T-ALL)[2] incited further study of the factors underlying circRNA dysregulation in this malignancy. An interesting lead to pursue was the observation that the splicing factor Quaking (QKI), previously linked to circRNA biogenesis[3,4], might be dysregulated in T-ALL. QKI is considered a tumor suppressor protein[5] and has reduced expression in solid cancer[6]. Less is known for leukemias. Heterogeneous *QKI* expression has been shown in B-cell ALL, with *QKI* downregulation in pediatric leukemias subtypes[7]. MiR-155-dependent-QKI depletion has been implicated in inflammation in chronic lymphocytic leukemia[8]. In T-ALL, *QKI* downregulation was reported in cases with high *HOXA* expression, carrying CALM-AF10[9] or *KMT2A* rearrangements[10]. The *QKI* transcript displayed a highly heterogeneous expression level in T-ALL (range: 0-15 TPM, **Figure 1a**), according to RNA-seq data in 25 pediatric patients[11] representing five T-ALL molecular subtypes[2].

Two groups of patients with normal (QKI_normal) and aberrantly low (QKI_low, **Figure 1a**) *QKI* expression were defined by comparison with their normal counterparts, five thymocyte populations from two healthy donors including three CD34+ early maturation and two CD4+CD8+ stages of the αβ lineage[2]. CircComPara2[12] identified 3 376 circRNAs expressed in the T-ALL samples, with an average of 5 circular isoforms per gene, 20 genes with at least 15 circular isoforms, including *TASP1* and *CASC15*, each with 30 circRNAs. A major effect of the T-ALL molecular subtypes on circRNA expression is known[2,9]. Since *QKI* expression is not independent of T-ALL molecular subtypes in this cohort (significant association between the *QKI* expression group and subtypes p-value<0.01), all statistical analyses of circRNA profiles in relation to *QKI* expression were conducted using the molecular subtypes as covariates to bring to light the net effect of *QKI* variation on circRNA expression level in T-ALL.

Unsupervised analysis of circRNA expression profiles showed that patient samples separate in a gradient coincident with increasing *QKI* levels (**Figure 1b**). The separation was less clear with the linear counterpart of circRNA-expressing genes and the circRNA expression variation in QKI_low vs. QKI_normal T-ALL was more marked than the variation of the linear counterpart (**Figure S1a-b**). We identified 209 circRNAs with expression significantly correlated with *QKI* level (Spearman's coefficient, |rho|>0.4, Benjamini-Hochberg, BH adj. p-value<0.05), 96 with positive and 113 negative correlation (**Figure 1c**), as exemplified by circUBAP2 and circMAN1A2, with a profile strongly directly and inversely correlated with *QKI* expression and high abundance.

Next, we examined the differences in circRNA expression among patient groups in relation to *QKI* level using multiple approaches, including machine learning techniques (DaMiRseq R package). Random Forest identified a subset of 149 circRNAs that classify T-ALL cases with low and normal *QKI* expression (**Figure 1d**). The importance of each circRNA in the classification model was prioritized using accuracy loss upon circRNA exclusion and circRNA contribution to the homogeneity of the nodes and leaves in the resulting Random Forest (Gini score; **Figure S1c**).

Regulatory activity at the splicing level is expected to result in a variation in both the absolute circRNA expression and the relative circRNA expression compared to the linear counterpart (circular to linear proportion, CLP). A varied absolute circRNA expression level, with a stable CLP across conditions, indicates indeed that the change in circRNA expression across conditions follows the linear expression pattern, being likely controlled at the transcriptional level. Instead, a CLP variation across conditions highlights an uncoupling of circRNA and linear expression variation.

The comparison of QKI_low with QKI_normal T-ALL circRNAomes identified 328 and 425 circRNAs with significantly varied (edgeR; robust estimation of dispersion; BH adj. p-value<0.1) expression (DE) and CLP (DP; CircTest[2]), respectively (**Figure 1e**). Considering absolute and relative circRNA expression, equal numbers of circRNAs were over- or less expressed in the QKI_low group (**Figure 1f** and **Table S1**). CircPHACTR4 was downregulated in link with QKI

reduced expression. For 133 and 37 circRNAs, respectively, a concordant significant increase and decrease in both expression level and CLP when comparing QKI_low with QKI_normal cases was recorded. CircRNAs with increased CLP and stable expression, like circRNAs derived from *SCRG1* and *FLG-AS1* genes (**Table S1**), indicated that QKI reduction may shift the equilibrium of circular and linear splicing in T-ALL. Importantly, 165 (28%) of the circRNAs with absolute or relative expression changes in the QKI_low group were previously found to be dysregulated in this malignancy[2], indicating that QKI abnormally low expression can explain, at least in part, circRNA dysregulation in T-ALL.

CircRNA modulated by the QKI level, highly expressed in T-ALL and dysregulated, in comparison with their normal counterparts, are shown in **Figure 1g**. CircRNAs upregulated in link with low QKI expression previously associated with oncogenic functions in other malignancies include circRTN4[13] and circTDRD3[14]. Overall, T-ALL patients stratified by QKI expression levels have different circRNAomes, with an abnormally reduced QKI level associated with a significant variation in absolute circRNA expression and a more marked change in the CLP.

Further data were obtained using QKI expression manipulation in T-ALL *in vitro*, choosing JURKAT cells with high endogenous QKI expression. About $4x10^6$ cells were transfected with 20 nM of NTC or QKI siRNA (ON-TARGETplus SMARTpool siRNA; Dharmacon®) using the Neon transfection system (Thermo Fisher). RNA was extracted 72 hours post-transfection (QIAGEN RNeasy Plus mini kit) and assessed for integrity. Efficiently silenced *QKI* (QKI_KD; **Figure 2a**) and control (CTR) RNA-seq profiling (Illumina Truseq stranded total RNA) showed that the global circRNA expression profile was affected by the *QKI* KD in T-ALL cells *in vitro* (**Figure 2b**). CircSUCO and circDNMT3B were among the most upregulated circRNAs upon *QKI* silencing, whereas circPHACTR4 and circKLHDC1 showed a dramatic reduction. Previous studies have reported that QKI favors the biogenesis of certain circRNAs[3]. However, equal numbers of circRNAs with an absolute expression increase (47.8%) and decrease (52.2%) upon *QKI* KD in T-

ALL *in vitro* were observed. Figures were similar considering only the 50% most abundant circRNAs and circRNAs with an absolute LFC higher than two (**Figure 2c**). These results are in line with a recent report that QKI knockout sustains the expression of certain circRNAs while suppressing others in mice cardiomyocytes.

Importantly, as we observed in patients, QKI silencing in T-ALL *in vitro* impacted the CLP, supporting the direct role of this protein in the regulation of the backsplicing efficiency. In most cases, the expression variation was associated with a varied CLP (**Figure 2d**), being thus uncoupled with the variation of the linear counterpart. There was a high concordance between circRNA expression and proportion variation. The majority (>80%) of circRNAs upregulated upon QKI KD also had an increased proportion, whereas only about half of the downregulated circRNAs also had a reduced CLP (**Figure 2d**). Isoform-specific regulation of alternative backsplicing was suggested by observation of circRNAs isoforms from the same gene with opposite behaviors upon QKI KD (**Figure S1d**). Moreover, we considered QKI-binding motifs (QKI response elements; QREs) residing in the introns adjacent (1000 bp) of back splice junctions, according to both CLIP-seq data (CLIPdb and starBase v2.0 databases) and QRE motif predictions (**Table S2**). QRE were enriched in the upstream flanking regions of downregulated circRNAs upon QKI KD and in downstream regions of upregulated circRNAs (Fisher's Exact Test, p-value = 0.049; **Figure 2e**). Expression changes, separating circRNAs with QRE downstream, upstream or on both sides confirmed this finding, also showing that a higher number of QRE associated with a larger expression variation (**Figure 2f**). Comparing our results in JURKAT cells with those previously observed in HEK293T cells[3], 540 circRNAs exhibited a concordant expression variation (absolute LFC at least 0.5) after QKI KD in both settings, implying causality. F.i. the abundance of circCAMSAP1, circSMARCA5, circPCMTD1 and circMGA with adjacent QKI PAR-CLIP sites was reduced following QKI knockdown in both datasets, corroborating our data.

Finally, considering 2 519 circRNAs expressed in both patients and JURKAT cells, a good concordance between the model and patient data emerged: 266 circRNAs were valuable features in model classification and had significant differential expression variation comparing QKI_low vs. QKI_normal T-ALL cases with a concordant variation of CLP or absolute expression upon QKI KD in T-ALL in vitro (**Figure 2g** and **Figure 3a**). Importantly, in the further comparison of QKI_low T-ALL with thymocytes from healthy donors, most of these circRNAs show significant dysregulation, consistent with the comparison in patient groups (**Figure 3a**).

CircTASP1 (chr20:13528433-13569586, exons 7-10 backspliced) and circPHACTR4 (chr1:28459085-28466535: exon 2-part of exon 5), respectively up- and down-regulated in QKI-reduced condition in T-ALL, and also with altered (8.2 times too high and 7.3 times too low) expression in QKI_low T-ALL compared with normal thymocytes underwent further investigation in KARPAS-45 and HBP-ALL and cell lines with respectively very low and high endogenous QKI expression. We obtained QKI silencing in HBP-ALL (85% reduction achieved). HEK293 cells were cotransfected with the envelope (pMD2.G), packaging (psPAX2) and the shRNA TRC vector (MISSION®, Sigma-Aldrich) harboring a shRNA non-targeting or targeting QKI (TRCN0000233373). HPB-ALL cells were transduced with viral particles (collected 72h and 96h post-transfection and concentrated 10 times using PEG-it; System Biosciences) by spinoculation (2300 rpm, 90 min, 32°C, 8 µg/mL polybrene H9268; Sigma-Aldrich). After 72 hours, 1 µg/mL of puromycin was included in the culturing media for the selection of transduced cells, for 7 days. We obtained also QKI overexpression in KARPAS-45 (90 times increase achieved), HEK293 cells were cotransfected with the envelope, packaging and a lentiviral vector harboring an ORF stuffer or the QKI ORF (pLV[Exp]-EF1A>ORF_Stuffer- CMV>Puro, VectorBuilder ID VB221221-1538ubv; pLV[Exp]-EF1A>hQKI[NM_006775.3]-CMV>Puro, VB221221-1535gjk). Viral production, transduction, selection and RNA extraction were performed as indicated above. Both experiments were performed 4 times. RT-qPCR was used to quantify circTASP1 and circPHACT4

(circTASP1_F, GTAGGCTCCTTCTCCAACTA; circTASP1_R, CCCAGGCTGCTCTTTATG; circPHACTR4_F, GAAGGGCAAGCAAAGGAT; circPHACTR4_R, GCTTGAAGATCTTGCCAAAG; iScript™ cDNA Synthesis Kit; BioRad SsoAdvanced Universal SYBR® Green Supermix; Roche LightCycler® 480; CellCarta QBase+ software for data analysis).

A significant increase of circTASP1 was observed upon QKI silencing in HBP-ALL cells (**Figure 3b**), corroborating the QKI dependency of this circRNA on QKI, with an indirect relation. CircTASP1 isoforms (exons 5-8, 4-7 and 8-10) are upregulated in T-ALL[2] and sustain acute myeloid leukemia (exons 4-6)[15].

CircPHACTR4 was markedly decreased upon QKI silencing also in HBP-ALL, as in JURKAT cells and increased upon QKI overexpression in KARPAS-45 cells (**Figure 3b**). Robust evidence was gathered of direct dependency of circPHACTR4 expression on the QKI level, concordantly in patients and in different T-ALL cell lines *in vitro.* CircPHACTR4 absolute decrease is uncoupled from the variation of the linear counterpart and is likely due to a post-transcriptional modulation. This isoform is derived from the tumor suppressor gene *PHACTR4* that also produces a tumor suppressor circRNA (circPHACTR4 chr1:28473553-28476291; exons 6-7)[16]. In the literature, QKI was described to favor circRNA biogenesis, whereas we showed that QKI reduction can affect different circRNAs groups in opposite ways, and provided experimental validation that QKI favors the expression of circPHACTR4 while suppressing circTASP1, suggesting a more complex picture.

In conclusion, T-ALL patients can be stratified by QKI expression and those with low QKI levels have a distinct circRNAome. In accordance with observations in patients, QKI silencing in T-ALL *in vitro* identified numerous circRNAs with QKI-dependent absolute and relative expression. We unveiled reduced QKI expression as a novel factor that could explain, at least in part, circRNA dysregulation in T-ALL.

References

1. Li Q, Ren X, Wang Y, Xin X. CircRNA: a rising star in leukemia. PeerJ. 2023;11:e15577.

2. Buratin A, Paganin M, Gaffo E, et al. Large-scale circular RNA deregulation in T-ALL: unlocking unique ectopic expression of molecular subtypes. Blood Adv. 2020;4(23):5902-5914.

3. Conn SJ, Pillman KA, Toubia J, et al. The RNA binding protein quaking regulates formation of circRNAs. Cell. 2015;160(6):1125-1134.

4. Gaffo E, Bonizzato A, Kronnie GT, Bortoluzzi S. CirComPara: A Multi-Method Comparative Bioinformatics Pipeline to Detect and Study circRNAs from RNA-seq Data. Noncoding RNA. 2017;3(1):8.

5. Chénard CA, Richard S. New implications for the QUAKING RNA binding protein in human disease. J Neurosci Res. 2008;86(2):233-242.

6. Bian Y, Wang L, Lu H, et al. Downregulation of tumor suppressor QKI in gastric cancer and its implication in cancer prognosis. Biochem Biophys Res Commun. 2012;422(1):187-193.

7. Bonizzato A, Gaffo E, Te Kronnie G, Bortoluzzi S. CircRNAs in hematopoiesis and hematological malignancies. Blood Cancer J. 2016;6(10):e483.

8. Tili E, Chiabai M, Palmieri D, et al. Quaking and miR-155 interactions in inflammation and leukemogenesis. Oncotarget- 2015;6(28):24599-24610.

9. Dik WA, Brahim W, Braun C, et al. CALM-AF10+ T-ALL expression profiles are characterized by overexpression of HOXA and BMI1 oncogenes. Leukemia. 2005;19(11):1948-1957.

10. Ferrando AA, Armstrong SA, Neuberg DS, et al. Gene expression signatures in MLL-rearranged T-lineage and B-precursor acute leukemias: dominance of HOX dysregulation. Blood. 2003;102(1):262-268.

11. Verboom K, Van Loocke W, Volders P-J, et al. A comprehensive inventory of TLX1 controlled long non-coding RNAs in T-cell acute lymphoblastic leukemia through polyA+ and total RNA sequencing. Haematologica. 2018;103(12):e585-e589.

12. Gaffo E, Buratin A, Dal Molin A, Bortoluzzi S. Sensitive, reliable and robust circRNA detection from RNA-seq with CirComPara2. Brief Bioinform. 2022;23(1):bbab418.

13. Wong CH, Lou UK, Fung FK-C, et al. CircRTN4 promotes pancreatic cancer progression through a novel CircRNA-miRNA-lncRNA pathway and stabilizing epithelial-mesenchymal transition protein. Mol Cancer. 2022;21(1):10.

14. Fu Z, Zhang P, Zhang R, et al. Novel hypoxia-induced HIF1α-circTDRD3-positive feedback loop promotes the growth and metastasis of colorectal cancer. Oncogene. 2023;42(3):238-252.

15. Lin Y, Huang Y, Liang C, Xie S, Xie A. Silencing of circTASP1 inhibits proliferation and induces apoptosis of acute myeloid leukaemia cells through modulating miR-515-5p/HMGA2 axis. J Cell Mol Med. 2021;25(15):7367-7380.

16. Wang Y, Yang Z, Gu J, et al. Estrogen receptor beta increases clear cell renal cell carcinoma stem cell phenotype via altering the circPHACTR4/miR-34b-5p/c-Myc signaling. FASEB J. 2022;36(2):e22163.

Figure legends

Figure 1. QKI shapes circRNA expression in T-ALL patients. a. QKI 5 nuclear transcript normalized expression in normal developing thymocytes allowed the definition of two groups (QKI-low, QKI_normal) of T-ALL (**, p-value≤0.01; ***, p-value≤0.001; ns, not-significant; Mann-Whitney Test). **b**. Unsupervised principal component analysis of circRNA expression profiles separated T-ALL patients (n=25) according to a gradient of *QKI* expression levels. **c**. Expression distribution of circRNAs negative, positive or none correlate with *QKI* expression in T-ALL patients; A table with total number, mean, and standard deviation (sd) for each subgroup of circRNAs defined by its correlation with *QKI* expression has been reported. **d**. Random forest classification analysis identified circRNAs well discriminating QKI_low and QKI_normal T-ALL for which the Heatmap shows standardized expression and other characteristics, such as Average expression across samples, length of the backsplice and circRNAs types. **e**. Manhattan plot of p-values from DE- and DP-circRNAs. Horizontal red lines indicate a p-value threshold of 0.1, highlighting the significant DE- and DP-circRNAs. DE-specific and DP-specific circRNAs are shown in green and pink, respectively. CircRNAs that are shared by DE and DS groups are shown in grey. **f**. Scatter plot of log Fold Change (FC) of significantly (p-value≤0.1) DE and DP circRNAs comparing QKI_low with QKI_normal T-ALL patients (x- and y-axis show the FC of respectively the CLP and absolute crcRNA expression). DE-specific and DP-specific circRNAs are shown in green and pink, respectively. CircRNAs that are both DE and DP are shown in grey. **g.** Scatterplot of circRNA log FC comparing QKI_low and QKI_normal T-ALL and circRNA average expression in T-ALL; 140 circRNAs significantly DE and DP and also among those discriminant between QKI_low vs QKI_normal T-ALL are shown; names are shown only for circRNAs with average expression at least 600 and absolute LFC at least 1 that were previously found dysregulated in T-ALL in[2].

Figure 2. CircRNA affected by QKI knock-down in T-ALL in vitro. a. QKI silencing in JURKAT cells (80% reduction in QKI_KD vs CTR). **b.** CircRNA expression separates QKI_KD from CTR samples (PCA based on 10,774 circRNA expression profiles). **c.** Barplot of the number of circRNAs binned by $\log_2$ Fold Change (logFC) absolute value comparing QKI_KD with CTR. The left and right sides represent the variation in absolute and relative expression, respectively. **d.** Sankey Plot of the intersections of circRNAs with Expression and/or CLP increased, decreased or unvaried upon QKI KD. **e.** QRE frequency in the introns flanking the back splice junctions. **f.** Scatterplot of logFC of circRNA expression variation in QKI_low vs. QKI_normal T-ALL patients (x-axis) and upon QKI KD in Jurkat cells (y-axis). Data are split according to the position of QRE detection in the flanking introns: only downstream, only upstream, or on both sides. The dots' color reflects the mean relative expression and size of the number of QRE detected in the flanking introns. logFC: log Fold Change. **g.** Mirror density plot of logFC of absolute (upper) and relative (bottom) expression variation upon QKI silencing in Jurkat cells and in QKI_low vs. QKI_normal T-ALL patients.

Figure 3. CircRNAs dependent from QKI expression in T-ALL. a. Heatmap of 35 circRNAs with concordant expression change in the KD experiment (absolute LFC>1 in QKI KD vs CTR) and significant absolute or relative (CLP) expression variation in QKI_low vs QKI_normal T-ALL; circRNAs are clustered according to LFC values; the LCF in the comparison between QKI-low T-ALL and normal thymocytes and adjusted p-value from the comparisons QKI_low vs QKI_normal T-ALL and QKI-low T-ALL vs thymocytes are also shown; estimated correlation with QKI expression level in T-ALL (rho); the discriminant property from Random Forest model in T-ALL QKI-group classification (Discriminant, YES or NO) and the average circRNA expression in T-ALL quantile (T-ALL Expr. Quantile, Q1-4). **b.** CircTASP1 and **c.** circPHACTR4 quantification by qRT-PCR in HPB-ALL cells upon QKI KD and in KARPAS-45 cells upon QKI overexpression (OE).

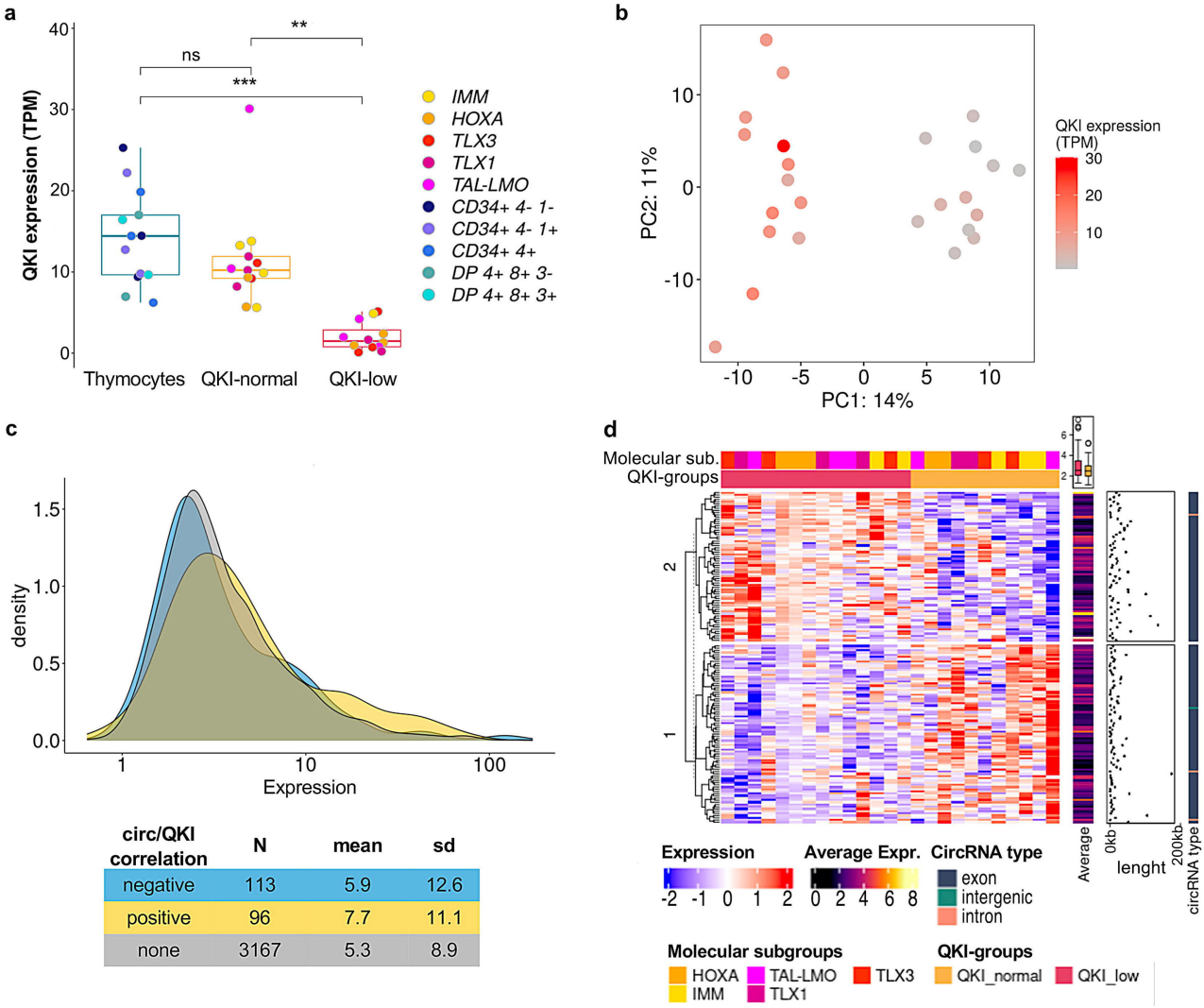

circ/QKI correlation	N	mean	sd
negative	113	5.9	12.6
positive	96	7.7	11.1
none	3167	5.3	8.9

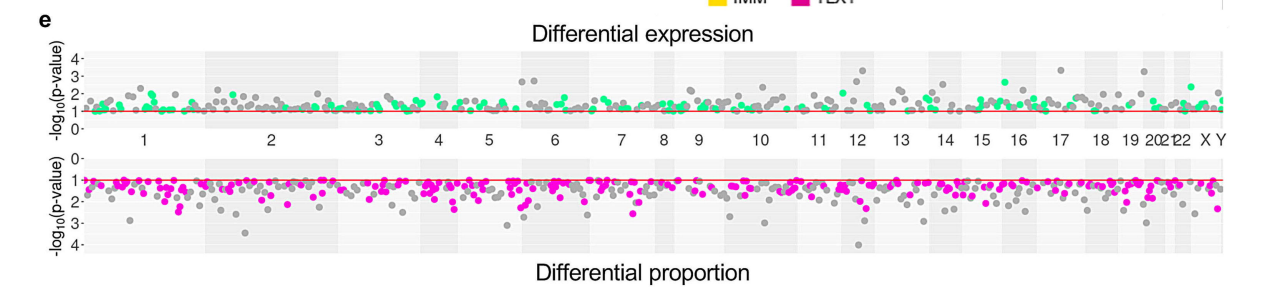

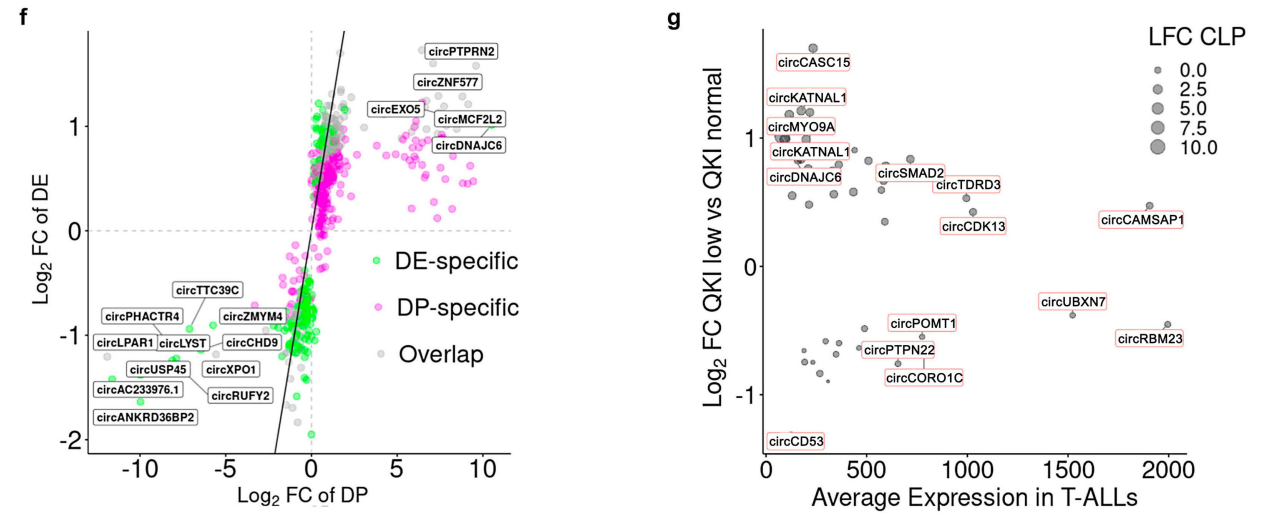

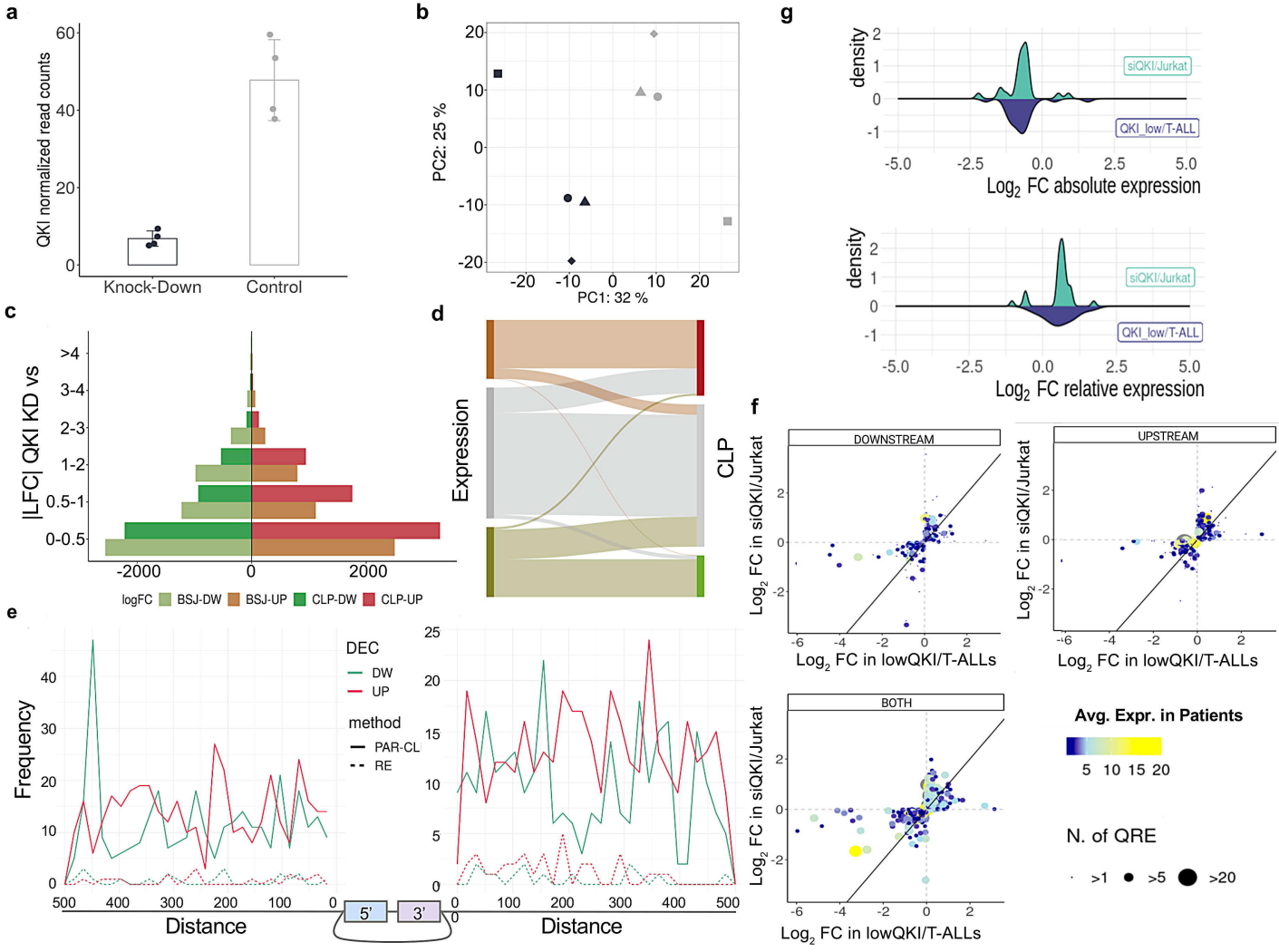
a
QKI normalized read counts
Knock-Down
Control
b
PC2: 25 %
PC1: 32 %
g
density
siQKI/Jurkat
QKI_low/T-ALL
Log2 FC absolute expression
Log2 FC relative expression
c
|LFC| QKI KD vs
logFC BSJ-DW BSJ-UP CLP-DW CLP-UP
d
Expression
CLP
f
DOWNSTREAM
UPSTREAM
BOTH
Log2 FC in siQKI/Jurkat
Log2 FC in lowQKI/T-ALLs
Avg. Expr. in Patients
N. of QRE
e
Frequency
DEC
DW
UP
method
PAR-CL
RE
Distance
5'
3'

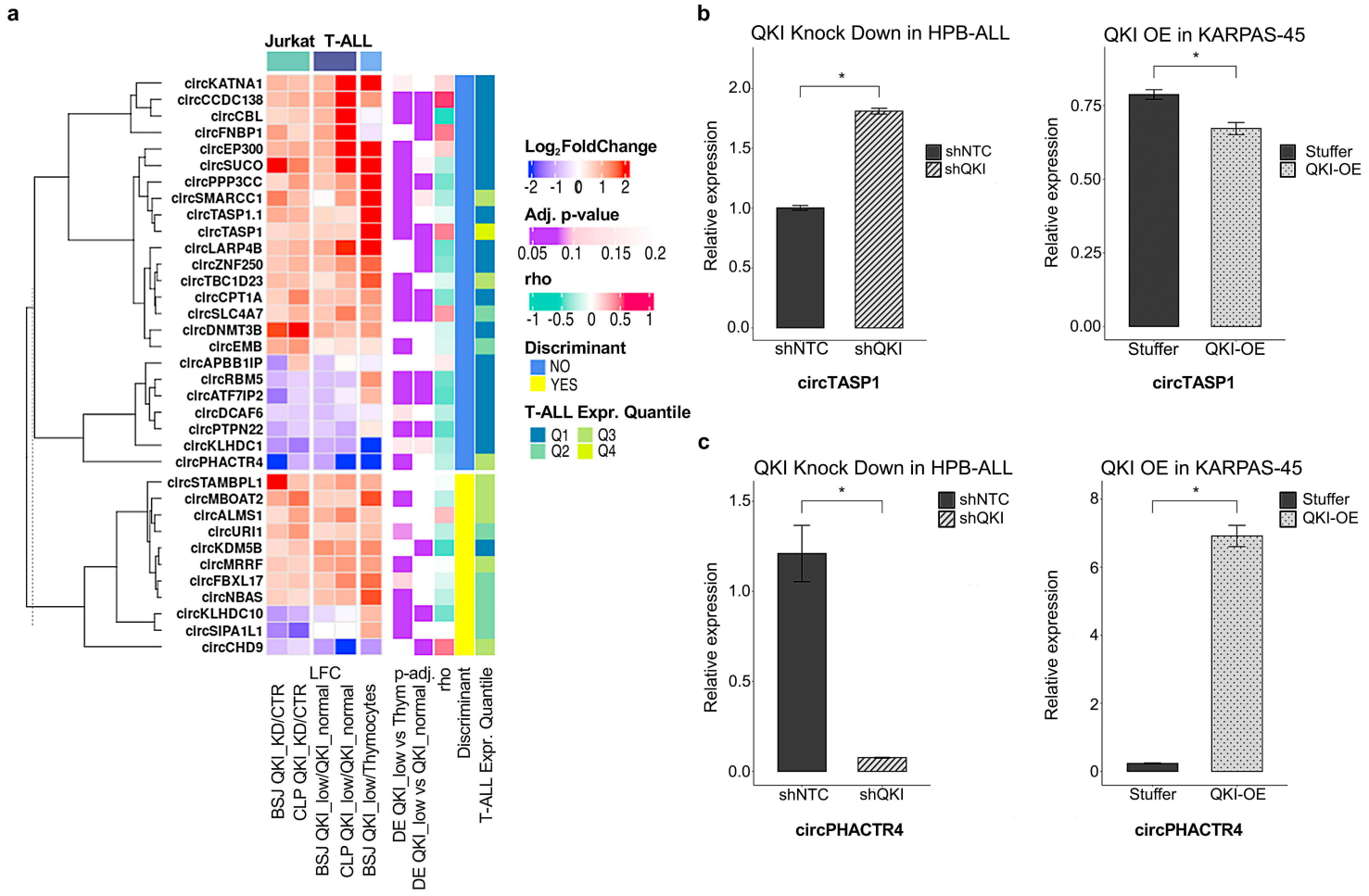
a
Jurkat T-ALL
circKATNA1
circCCDC138
circCBL
circFNBP1
circEP300
circSUCO
circPPP3CC
circSMARCC1
circTASP1.1
circTASP1
circLARP4B
circZNF250
circTBC1D23
circCPT1A
circSLC4A7
circDNMT3B
circEMB
circAPBB1IP
circRBM5
circATF7IP2
circDCAF6
circPTPN22
circKLHDC1
circPHACTR4
circSTAMBPL1
circMBOAT2
circALMS1
circURI1
circKDM5B
circMRRF
circFBXL17
circNBAS
circKLHDC10
circSIPA1L1
circCHD9
Log2FoldChange
-2 -1 0 1 2
Adj. p-value
0.05 0.1 0.15 0.2
rho
-1 -0.5 0 0.5 1
Discriminant
NO
YES
T-ALL Expr. Quantile
Q1 Q3
Q2 Q4
LFC
p-adj.
rho
Discriminant
T-ALL Expr. Quantile
BSJ QKI_KD/CTR
CLP QKI_KD/CTR
BSJ QKI_low/QKI_normal
CLP QKI_low/QKI_normal
BSJ QKI_low/Thymocytes
DE QKI_low vs Thym
DE QKI_low vs QKI_normal
b
QKI Knock Down in HPB-ALL
Relative expression
shNTC
shQKI
circTASP1
QKI OE in KARPAS-45
Stuffer
QKI-OE
circTASP1
c
QKI Knock Down in HPB-ALL
circPHACTR4
QKI OE in KARPAS-45
circPHACTR4

Depletion of the RNA binding protein QKI shapes circular RNA dysregulation in T-cell acute lymphoblastic leukemia

Alessia Buratin[1], Bruno Palhais[2,3,4], Enrico Gaffo[1], Juliette Roels[4], Julie Morscio[4], Jolien Van Laere[4], Silvia Orsi[1,5], Geertruij te Kronnie[1], Pieter Van Vlierberghe[4], Panagiotis Ntziachristos[2,3,4] and Stefania Bortoluzzi[1*]

[1] Department of Molecular Medicine, University of Padova, Padova, Italy

[2] Leukemia Therapy Resistance Unit, Department of Biomolecular Medicine, Ghent University, Ghent, Belgium.

[3] Center for Medical Genetics, Ghent University and University Hospital, Ghent, Belgium.

[4] Cancer Research Institute Ghent (CRIG), Ghent, Belgium

[5] Department of Biology, University of Padova, Padova, Italy

***Correspondence:** Prof. Stefania Bortoluzzi, Department of Molecular Medicine, University of Padova, via G. Colombo 3, 35131- Padova, Italy. Email: stefania.bortoluzzi@unipd.it

Supplementary Results

Figure S1. a. Unsupervised principal component analysis of T-ALL patients (n=25) according to expression profiles of the circRNA linear counterpart (overlapping mRNAs in circRNA-expressing genes; Samples are colored according to a gradient of *QKI* expression levels); b. Scatter plot of expression log Fold Change of circRNAs and their linear counterpart when comparing QKI_low with QKI_normal T-ALL; c) CircRNAs importance plot in the Random Forest classification model of QKI_low and QKI_normal T-ALL samples (Gini index and Accuracy measure were used to rank the most discriminating circRNAs; Dots are colored according to Adj. p-value significance; Names are reported for the top 6 circRNAs); d) Boxplot of circRNA isoforms expressed from the same host gene and with opposite behavior upon QKI KD in Jurkat cells.

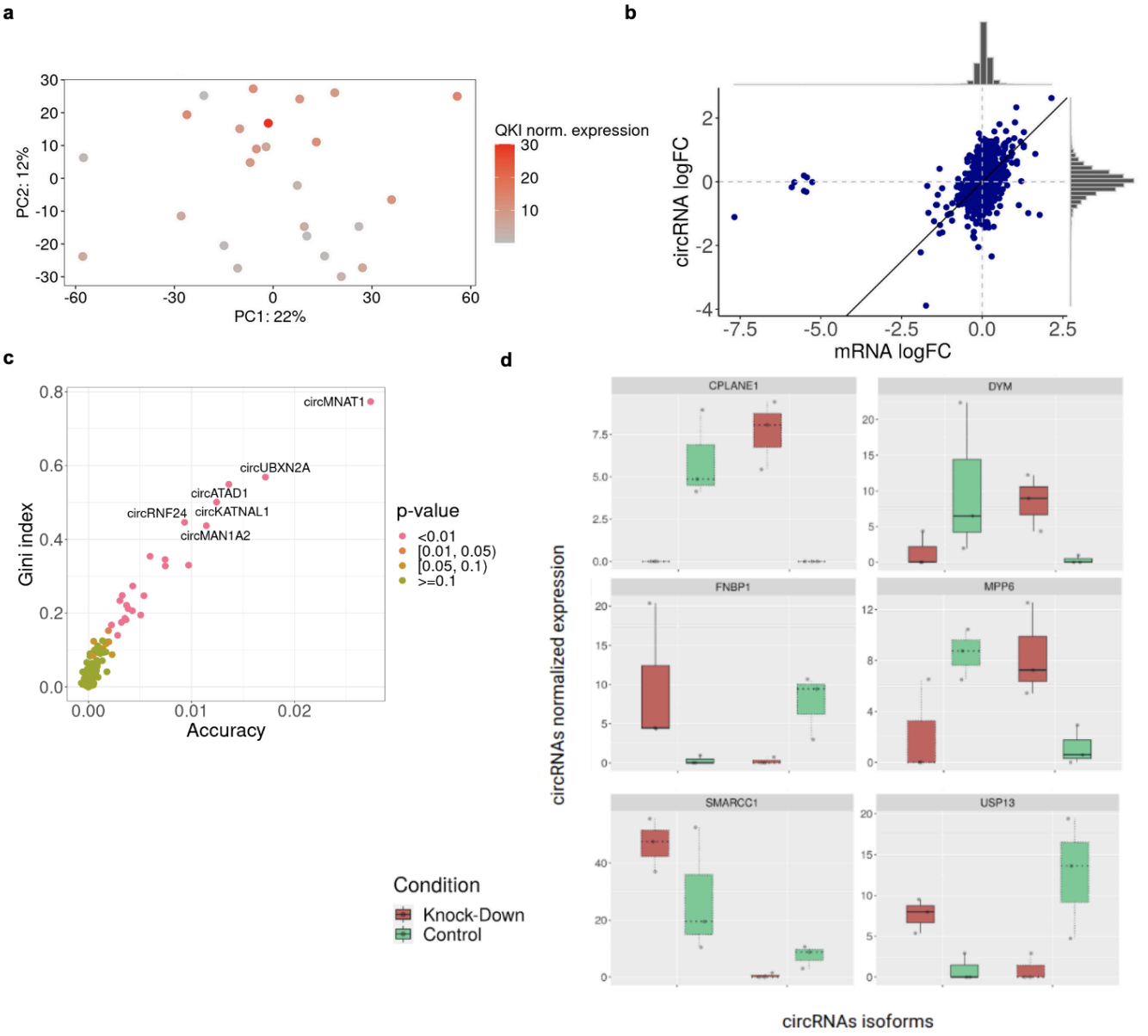

Table S1. Table of 3 376 circRNAs used to compare T-ALL patients with low QKI and with normal expression level (QKI_low vs QKI_normal). For each circRNAs are reported the host gene info; absolute (.EXP) and relative (.CLP) average expression; statistical test and p-value of the QKI-subgroups comparison for absolute and relative expression, respectively.

(see file .xls)

Table S2. QKI response elements coordinates from PAR-CLIP experiment or predicted by using regular expression within 1000 nt upstream or downstream of the circRNAs backsplice sites detected in QKI Knock-Down experiment in Jurkat cells. The distance from the backsplice junction and the position (Upstream/Downstream) relative to the backsplice are also reported. For predicted QRE the string is reported in the last column.

(see file .xls)